ISSN (Print) 1226-1750
ISSN (Online) 2233-6656
Journal of Magnetics 27(2), 201-209 (2022) https://doi.org/10.4283/JMAG.2022.27.2.201

Estimation of Optimum Flip Angle using 3D VANE XD Technique: Focused on Pre-Contrast and Hepatobiliary Phase

Eun-Hoe Goo*

Department of Radiological Science, Cheongju University, Cheongju, Chungbuk 28503, Republic of Korea

(Received 17 February 2022, Received in final form 15 April 2022, Accepted 9 May 2022)

To investigate the optimum flip angle that can enhance image quality, SNR (signal to noise ratio), and CNR (contrast to noise ratio), comparing the images obtained, applying flip angles, 11°, 14°, 17°, 20°, and 23° in getting Liver Hepatobiliary Phase image using 3D VANE XD(3D Multivane mDixon, Philips Healthcare) technique. Experiments were conducted on a total of 30 outpatients and inpatients to our hospital (HCC:10, Metastasis:10, Abscess:10). As for the equipment used in the experiments, Philips Ingenia 3.0T CX was used, and all parameters other than the flip angle were set the same to conduct the tests. As for the image analysis method, using the Image-J program (National Institutes of Health and LOCI), the SNR of the liver, kidney, and pancreas obtained from the images by flip angle before the contrast medium injection and the CNR between the lesion and the normal tissue after the contrast medium injection were measured to conduct comparative analysis. As a result of a comparison of images before and after the contrast medium injection by disease, when the flip angle of 17° was applied, SNR and CNR were measured higher than in the images of other flip angles ($p<0.05$). In the comparisons of the images taken before and after the injection of contrast medium by disease, when a flip angle of 17° was applied, the SNR before contrast medium injection was 28-29 % higher, and the SNR after the injection of contrast medium was 11 % up to 49 % higher than that at other flip angles. There was a difference in CNR before contrast medium injection of 30-43 % and CNR after contrast medium injection of 58-68 %. The measured value increased up to 17° and then decreased after that. Additionally, in the qualitative evaluation, Lesion Conspicuity ($p=0.003$), Image Artifact ($p=0.0001$), Lesion Delineation ($p=0.0002$), and Vascular Anatomy ($p=0.0002$) received the most excellent evaluations at 17°. In conclusion, in this study, the flip angle of 17° provided the highest SNR and CNR values when the tests were conducted using the free breath hold technique, 3D VANE XD Sequence. Thus, in liver MRI protocol tests, the overall diagnostic information was provided, including hypervascular tumor.

Keywords : flip angle, 3D VANE XD, Image J, hepatobiliary phase

1. Introduction

South Korea is one of the countries with high liver-related diseases or morbidity, and the important cause of death among adults in their 40s and 50s, who are the most socially productive is also liver disease [1]. MRI is used when it is difficult to detect a liver lesion discovered in ultrasound or CT or when it is necessary to make an accurate decision on the clinical stage of hepatocellular carcinoma [2, 3]. In addition, it has advantages that it has more excellent soft tissue contrast compared to CT and does not have any biological risk related to radiation; however, it has demerits that it takes much time and is weak to the patient's motion [4]. 3D T1 Gradient Echo (GRE) abdomen image has excellent Signal to Noise Ratio (SNR) and is an important imaging modality in discovering the topical lesion of the liver and understanding the characteristics [5]. SNR is affected by several parameters and can be shown as the following equation (Eq. 1).

$$\text{SNR} \propto \text{voxel volume} \times \sqrt{\text{acqustition time}}\,, \quad (1)$$

Thus, the relationship between Scan Parameters and SNR can be drawn up like the following equation (Eq. 2).

$$\text{SNR} \propto \frac{FOV_x}{N_x} \times \frac{FOV_y}{N_y} \times \text{slice thickness} \times \sqrt{\frac{N_x N_x N_{ave}}{RBW}}\,. \quad (2)$$

Prior to the description of 3D T1 GRE, it is necessary

*Corresponding author: Tel: +82-043-229-7994
Fax: +82-043-229-7947, e-mail: gooeh@cju.ac.kr

to describe Flip Angle (FA) and MRI signal intensity. To obtain an MRI image, the process of transforming longitudinal magnetization into transverse magnetization with RF Pulse is required, and at this time, longitudinal magnetization energy changing into a certain angle is called excitation, and the angle of change is called flip angle [7]. The flip angle is determined by the proton's gyromagnetic ratio, gradient echo intensity, and the time of applied resonance frequency, which is like the following equation (Eq. 3).

$$\theta = \gamma \cdot B_1 \cdot t \tag{3}$$

θ: Flip angle,
γ: Gyromagnetic ratio,
B_1 : The gradient strength of the field B_1,
t : Time duration.

Where FA is one of the factors determining the contrast of the image. The greater FA, the more the volume of the longitudinal magnetization transversely. At this time, according to the TR value and relaxation time of the tissue, the contrast of the image changes, and the 3D T1 GRE image uses a flip angle less than 90°. FA producing the maximum signal intensity according to the given TR and T1 relaxation time is called Ernst Angle, and it is like the following equation (Eq. 4) [8].

$$S = A \sin\alpha \frac{1 - \exp\left(-\frac{TR}{T_1}\right)}{1 - \cos\alpha \exp\left(-\frac{TR}{T_1}\right)} \tag{4}$$

S : Signal intensity
A : The maximum signal amplitude of the spoiled gradient echo.

Breath Hold (BH) 3D T1 GRE technique can get steady images with a single breath holding; however, Motion Artifact occurs unless the patient holds breath due to a long test time [9, 10] (Fig. 1).

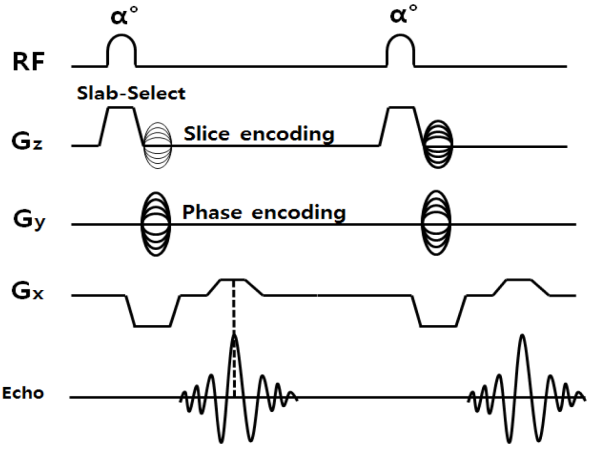

Fig. 1. 3-dimensinal spoiled gradient echo pulse sequence diagram[9] and Liver eTHRIVE image.

The 3D VANE XD technique, developed by Philips (Royal Philips Electronics N. V, Netherlands) uses radial sampling instead of Cartesian sampling in the existing BH method as the method for collecting K-Space data, which can conduct an abdominal examination with Free Breathing (FB) [11] (Fig. 2).

Since the FFT algorithm is implemented in the Cartesian coordinate system, it is impossible to apply that to the raw data obtained unevenly by radial sampling. Thus, using

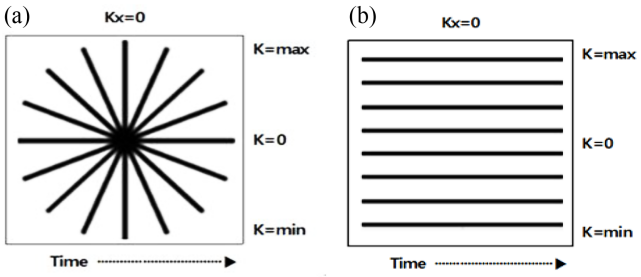

Fig. 2. K-Space Sampling Diagram. Illustration the Cartesian Sampling Scheme (a) and Radial Sampling Scheme (b).

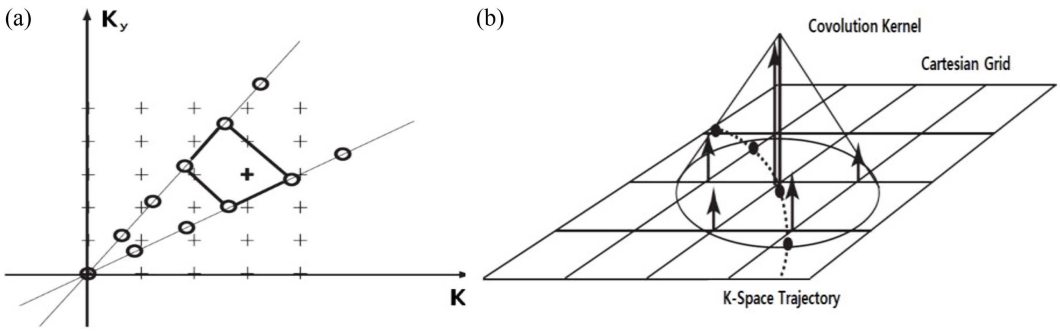

Fig. 3. Illustration determine the Value of the Catesian Samples through the adjacent samples from the Radial acquisition. (a) is Interpolating Cartesian Data points from Radial acquisition, (b) is Gridding Kernel Convolution and Resampling.

the gridding reconstruction algorithm, radial data are made even with the density-corrected function, and the gridding kernel function is calculated to convert that to the Cartesian coordinate system so that the image is reconstructed with the below equation (Eq. 5) through FFT (Fig. 3).

$$F_g = [(FSW) \otimes C]\,\mathrm{R}. \quad (5)$$

F_g : The data after gridding,
S : Series of delta function in K-Space,
W : A sampling density weighting correction applied to the delta functions,
C : Convolution kernel used for gridding,
R : Rectangular grid,
$\otimes$: Convolution operator.

For Cartesian sampling, some data filling the center of K-Space affect the SNR and contrast of the entire image while for radial sampling, since the obtained data are concentrated in the center, it can be calibrated even if an artifact occurs in some data, which is very effective for motion artifacts. Primovist® (Bayer, Germany), universally used in a liver MRI scan is Gadolinium-Ethoxybenzyl-Diethylenetriamine Pentaacetic Acid (Gd-EOB-DTPA) ingredient, and because of its property that it is discharged through the kidney earlier and through the liver later after in vivo injection, which is a medicine with the characteristics of non-specific extracellular contrast medium and hepatocyte-specific contrast medium. Thus, since it can get Hepato-Biliary Phase (HBP) images through morphological characteristics and hepatic excretion, it has an advantage that the functional information can also be known [13]. Hepato-Cellular Carcinoma (HCC) can be diagnosed by the observation of wash-out images in the artery phase, portal phase, and hepatobiliary phase in hepatocyte-specific contrast medium MRI scans. Generally, an HBP image is obtained 20 minutes after the contrast medium injection, and with strong hepatic parenchymal contrast enhanced, it can enhance diagnostic sensitivity with very excellent contrast of the liver lesion and hepatic parenchyma [14]. BH 3D T1 GRE image is a test method for which the patient's cooperation is important and has a disadvantage that it is impossible to proceed with the test if the patient is unconscious or cannot suppress breath due to auditory disorder, etc. [15]. Also, in an HBP scan, FA of GRE Pulse has a different initial set value according to the MRI equipment of each manufacturer, and to the author's knowledge, most studies of the optimum FA have used the respiratory standstill method, and there have been no reports on free-breath hold. Thus, this study applied different FAs (11°, 14°, 17°, 20°, and 23°) of images before and after the contrast medium injection to hypovascular diseases like hepatocellular carcinoma, abscess, and metastasis with 3D VANE XD technique and looked for the optimum FA through quantitative and qualitative evaluations of each image to provide the patients who could not have the test due to the breath issue with diagnostic information including a hypervascular tumor in liver MRI protocol test based on that.

2. Subjects and Method

2.1. Subjects

As for data in this study, using Ingenia 3.0T CX equipment (Philips Healthcare, Netherlands), from May 2019 through July 2021, with a total of 90 persons (46 men, 44 women, average age: 62.5 ± 13.56), images were analyzed, transmitting data of (HCC: 30 persons, Liver Metastasis: 30 persons, Abscess: 30 persons) to PACS (INFINITT Healthcare). All patient data were approved by the Subcommittee of Institutional Bioethics Committees of Cheongju University, concerning the patient data (IRB NO. 104407-202204-HR-001-01).

As for the data acquisition method, unlike the basic method, the image before the contrast medium injection and the image taken 20 minutes after injection, were acquired, using 3D VANE XD Pulse sequence while inducing breath. As for the parameters, all but FA were set the same, while a test of FA was conducted from 11° to 23° at an interval of 3°. The parameters used in this study are like Table 1.

2.2. Contrast media

An automatic injector (Autoinjector, Dual Autoinjector, Wlrichmedial, USA) was employed for the injection of contrast medium, and at an injection speed of 1 mL/sec., 10 mL of it was injected in total. As a contrast medium, Gadolinium contrast medium (Gd-EOB-DTPA; Primovist®,

Table 1. Scanning Parameters for 3D VANE XD.

Parameters	3D VANE XD		
TR (ms)[a)]	4.7		
TE (ms)[b)]	1.37		
Slice Thickness (mm)	3		
Gap (mm)	Default		
NEX	1		
Matrix	252 × 252		
FOV (mm)	380 × 380		
Flip Angle (°)	11°, 14°, 17°, 20°, 23°		
Scan Time	11°, 14°, 17° (2 min 13 sec)	20° (2 min 15 sec)	23° (2 min 18 sec)

[a)]TR: Radio-Frequency iteration cycle (repetition Time), [b)]TE: signal collection time (echo Time).

Schering, Berlin, Germany) was used.

2.3. Analysis method

With the acquired images, quantitative evaluation and qualitative evaluation were conducted. First, as a quantitative evaluation, with Digital Imaging and Communications in Medicine (DICOM) file transmitted to PACS, SNR and CNR were measured and analyzed with Image J (Ver. 1.52p, National Institutes of Health and LOCI) program. Hepatic parenchyma, lesion and background noise signal intensity were measured at the same position of the same cross-section after setting Region Of Interest (ROI). As for the position of ROI, the biggest possible ROI was set in the lesion and the surrounding normal hepatic parenchyma, avoiding the regions with artifacts by large blood vessels or movements. For the signal intensity of the background noise, setting ROI on the front and rear space of the abdomen surface in the phase encoding direction, SNR and CNR were calculated by checking the quantitative values with the following equations (Eqs. 6, 7).

$$\mathrm{SNR} = \frac{SI_{\mathrm{measurement}} \times 0.655}{\sigma_{\mathrm{backgroundnoise}} \times \sqrt{\mathrm{scan\ time}}}, \quad (6)$$

$$\mathrm{CNR} = \frac{(SI_{\mathrm{measurement}} - SI_{\mathrm{adjacent}}) \times 0.655}{\sigma_{\mathrm{backgroundnoise}} \times \sqrt{\mathrm{scan\ time}}}, \quad (7)$$

For qualitative evaluation, through the interpreter's sight, the scores for lesion conspicuity, imaging artifact, lesion delineation, and vascular anatomy were leveled off and compared, which were obtained by dividing them into five levels, Unacceptable (1), Poor (2), Fair (3), Good (4), and Excellent (5) under an agreement of two radiologists (One radiologist with more than 10 years' experience and one international MRI radiologist with more than 20 years).

2.4. Statistic analysis

As for quantitative analysis, for a comparison of flip angles, an ANOVA was conducted. As a post-hoc test, the Bonferroni method was used for calculation. Significance was given when the p-value was less than 0.05. As for qualitative analysis, as the evaluation of image quality, Kruskal-Wallis Test was used. Cohen's kappa analysis (0.8-0.9) was conducted to estimate the accuracy of the observer for the Region Of Interest (ROI). PASW Statistics (release 23.0) was used as a statistics program applied in this study.

3. Results

3.1. SNR result

For a total of 90 persons used in this analysis of image data, a certain ROI was set, and SNR was measured by analyzing the data on the live, kidney, pancreas, and spleen of the image before the contrast medium injection and HBP image at flip angles of 11°, 14°, 17°, 20°, and 23°. The mean and standard deviation values of the image before the contrast medium injection were as follows: Liver (23.9 ± 4.33, 24.96 ± 3.12, 31.73 ± 5.59, 24.08 ± 4.37 & 18.83 ± 1.40), Kidney (20.49 ± 2.72, 21.13 ± 1.89, 27.86 ± 9.15, 17.04 ± 4.04 & 14.54 ± 3.43), Pancreas (29.77 ± 6.24, 28.04 ± 5.78, 35.79 ± 8.24, 26.61 ± 5.97 & 23.25 ± 2.95), and Spleen (19.21 ± 3.86, 19.77 ± 2.28,

Table 2. Results of quantitative analyses: SNRs of pre-contrast image using five flip angles.

	11°	14°	17°	20°	23°	p1	p2
Liver	23.91 ± 4.33	24.96 ± 3.12	31.72 ± 5.59	24.08 ± 4.37	18.83 ± 1.40	0.0001	0.0001
Kidney	20.49 ± 2.72	21.13 ± 1.89	27.86 ± 9.15	17.04 ± 4.04	14.54 ± 3.43	0.0001	0.0001
Pancreas (Body)	29.77 ± 6.24	28.04 ± 5.78	35.79 ± 8.24	26.61 ± 5.97	23.25 ± 2.95	0.0001	0.0001
Spleen	19.21 ± 3.86	19.77 ± 2.28	25.05 ± 6.98	16.23 ± 2.74	15.29 ± 2.91	0.0001	0.0001

Note: Numbers are mean ± standard deviation.
ANOVA test (p1), Post-Hoc Test Bonferroni Correction (p2), $p<0.001$.

Table 3. Results of quantitative analyses: SNRs of hepatobiliary phase image using five flip angles.

	11°	14°	17°	20°	23°	p1	p2
Liver	115.00 ± 11.69	94.73 ± 15.65	143.63 ± 16.16	125.31 ± 14.39	105.55 ± 12.71	0.0001	0.0001
Kidney	97.70 ± 8.35	68.43 ± 7.75	113.83 ± 14.79	94.95 ± 5.70	69.77 ± 10.38	0.0001	0.0001
Pancreas (Body)	80.45 ± 8.36	57.76 ± 7.89	75.81 ± 9.30	62.23 ± 8.09	48.31 ± 6.56	0.0001	0.0001
Spleen	60.81 ± 8.07	44.33 ± 7.6	63.02 ± 7.38	54.76 ± 5.67	44.82 ± 7.51	0.0001	0.0001

Note: Numbers are mean ± standard deviation.
ANOVA test (p1), Post-Hoc Test Bonferroni Correction (p2), $p<0.001$.

25.05 ± 63.98, 16.23 ± 2.74 & 15.29 ± 2.91) (Table 2, p<0.05). The mean and standard deviation values of the HPB image, measured 20 minutes after the contrast medium injection were as follows: Liver (115.00 ± 11.69, 94.73 ± 15.56, 143.63 ± 16.16, 125.31 ± 14.39 & 105.55 ± 12.71), Kidney (97.70 ± 8.35, 68.43 ± 7.75, 113.83 ± 14.79, 94.95 ± 5.70 & 69.77 ± 10.38), Pancreas (80.45 ± 8.36, 57.76 ± 7.89, 75.81 ± 9.30, 62.23 ± 8.09 & 48.31 ± 6.56), and Spleen (60.81 ± 8.07, 44.33 ± 7.60, 63.02 ± 7.38, 54.76 ± 5.67 & 44.82 ± 7.51) (Table 3, p<0.05). Overall, it was found that SNR values differed depending on changes in the five flip angles (P<0.05). As a result of a comparison of SNR of images before and after the contrast medium injection, the more the flip angle, the higher SNR became, and it tended to decrease after 17°.

3.2. CNR result

HCC, Liver Metastasis, and Liver Abscess were selected as the target diseases, measurements were made by setting ROI on the normal region closest to the region of the lesion in the hepatic parenchyma. CNR was measured with the same method for SNR measurement by disease for the image before the contrast medium injection and HBP image after 20 min. In abdominal MRI images, the mean and standard deviation values of CNR in the imaged before the contrast medium injection in the liver, kidney, pancreas, and spleen were as follows: HCC (10.64 ± 4.11, 10.78 ± 4.34, 15.29 ± 5.13, 11.76 ± 5.09 & 8.77 ± 4.36), Metastasis (11.34 ± 5.17, 13.36 ± 6.36, 16.64 ± 7.18, 13.24 ± 5.31 & 10.36 ± 5.89), and Abscess (10.62 ± 6.87, 11.45 ± 6.32, 14.54 ± 7.16, 12.57 ± 5.31 & 11.36 ± 4.89) (Table 4, Fig. 4, p<0.05); and the mean and standard deviation values of HBP images were as follows: HCC (57.12 ± 5349, 51.00 ± 9.37, 92.23 ± 11.34, 82.19 ± 10.68 & 81.08 ± 9.64), Metastasis (49.36 ± 11.78, 50.37 ± 10.69, 86.19 ± 13.48, 79.71 ± 9.56 & 75.12 ± 7.11), and Abscess (55.64 ± 11.36, 51.28 ± 13.77, 79.17 ± 15.36, 70.49 ± 14.78 & 69.36 ± 13.26) (Table 5, Fig. 5, p<0.05). The results of the measurement of CNR were the same as those of SNR, and the measurement values were the highest in the image at 17°.

3.3. Results of qualitative analysis

The qualitative analysis standardized and compared the

Table 4. Results of quantitative analyses: CNRs of precontrast image using five flip angles.

	11°	14°	17°	20°	23°	p1	p2
HCC	10.64 ± 4.11	10.78 ± 4.34	15.29 ± 5.13	11.76 ± 5.09	8.77 ± 4.36	0.0001	0.0001
Metastasis	11.34 ± 5.17	13.36 ± 6.36	16.64 ± 7.18	13.24 ± 5.31	10.36 ± 5.89	0.0001	0.0001
Abscess	10.62 ± 6.87	11.45 ± 6.32	14.54 ± 7.16	12.57 ± 5.31	11.36 ± 4.89	0.0001	0.0001

Note: Numbers are mean ± standard deviation.
ANOVA test (p1), Post-Hoc Test Bonferroni Correction (p2), p<0.001.

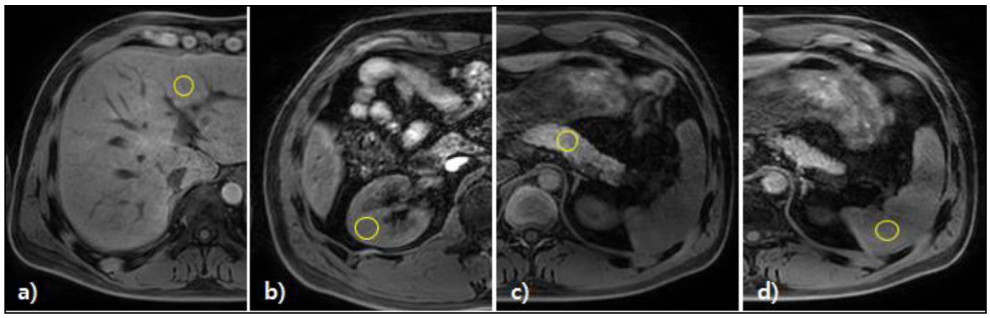

Fig. 4. (Color online) Precontrast images for Liver, Kidney, Pancreas, and Spleen in abdominal MRI images. In all images (a, b, c, and d), SNR and CNR were the highest at FA 17°.

Table 5. Results of quantitative analyses: CNRs of hepatobiliary phase image using five flip angles.

	11°	14°	17°	20°	23°	p1	p2
HCC	57.12 ± 5.49	51.00 ± 9.37	92.23 ± 11.34	82.19 ± 10.68	81.08 ± 9.64	0.0001	0.0001
Metastasis	49.36 ± 11.78	50.37 ± 10.69	86.19 ± 13.48	79.71 ± 9.56	75.12 ± 7.11	0.0001	0.0001
Abscess	55.64 ± 11.36	51.28 ± 13.77	79.17 ± 15.36	70.49 ± 14.78	69.36 ± 13.26	0.0001	0.0001

Note: Numbers are mean ± standard deviation.
ANOVA test (p1), Post-Hoc Test Bonferroni Correction (p2), p<0.001

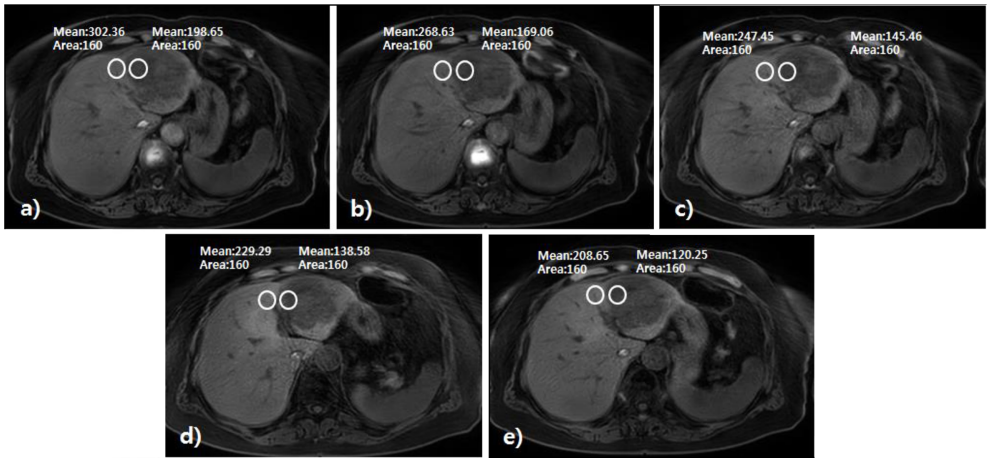

Fig. 5. 3D-mDixon HBP images with HCC according to Five Flip Angle of 11° (a), 14° (b), 17° (c), 20° (d) and 23° (e). On axial planes, the signal intensity in 3D-mDixon image at FA of 17° (c) is the highest of others images (11° (a), 14° (b), 20° (d) and 23° (e).

Table 6. Qualitative analysis: lesion conspicuity, imaging artifact, lesion delineation, vascular anatomy at each flip angle.

	11°	14°	17°	20°	23°	p1
Lesion Conspicuity	3.62 ± 0.98	3.15 ± 0.89	4.28 ± 1.23	3.63 ± 1.05	3.41 ± 0.94	0.0003
Image Artifact	3.12 ± 0.78	3.81 ± 0.77	4.16 ± 0.89	3.22 ± 0.73	3.65 ± 0.74	0.0001
Lesion Delineation	3.25 ± 1.07	3.11 ± 0.91	3.98 ± 1.31	3.26 ± 1.09	3.09 ± 0.98	0.0002
Vascular Anatomy	3.17 ± 1.11	3.32 ± 0.91	4.3 ± 1.29	3.17 ± 1.27	3.29 ± 1.03	0.0002

Note: Numbers are mean ± standard deviation.
Kruskal-Wallis H test (p1), $p<0.001$).

scores obtained on a five-point scale for four items, including lesion conspicuity, delineation, imaging artifact, and vascular anatomy. In five images by Flip Angle, most of the scores of the qualitative analysis were more than three points (Fair) and the scores were more than four points (Good) for all items in the image at 17°, which were good for the use as a diagnostic test (Table 6). Figure 6 shows the images obtained from five flip angles for HCC (arrow), Metastasis (elliptical), and Abscess (Arrowhead) before the contrast medium injection with the BH technique. The image on the first row (arrow) is that of a 68-year-old woman, a patient who received a definite diagnosis with HCC by an MRI scan as a 6 cm mass was observed on abdominal ultrasound and CT. The image on the middle row (elliptical) is that of a 59-year-old man, who is a Sigmoid Cancer patient, for whom an MRI scan was conducted since liver metastasis was observed in a CT scan. The image on the line on the bottom row (Arrowhead) is that of a 59-year-old man, who was tested since he was suspected of liver abscess in another hospital with right epigastric pain since a week before the visit. For the visual observations of the images by disease, since relatively more motion artifacts occurred in the images at 11° and 14° compared to those in the other experimental groups, they were evaluated to have poor blood vessel and lesion delineation in the hepatic parenchyma while in the images at 20° and 23°, the image density tended to decline. In contrast, the image at 17° was little affected by Motion Artifact and had high evaluation in the anatomical description of internal structures as well.

As a result of quantitative and qualitative analyses of data in this experiment, when SNR and CNR of each Flip Angle image were measured and compared, in both the image before the contrast medium injection and the image at a delay time of 20 min. after the injection of hepatocyte-specific contrast medium, SNR and CNR were the highest at the flip angle of 17° and excellent also in the qualitative analysis.

4. Discussion

One of the important advantages of abdominal MRI is that it can get a strong contrast-enhanced image of the organ to check as the contrast medium has been developed, which is selectively accumulated in the specific organ

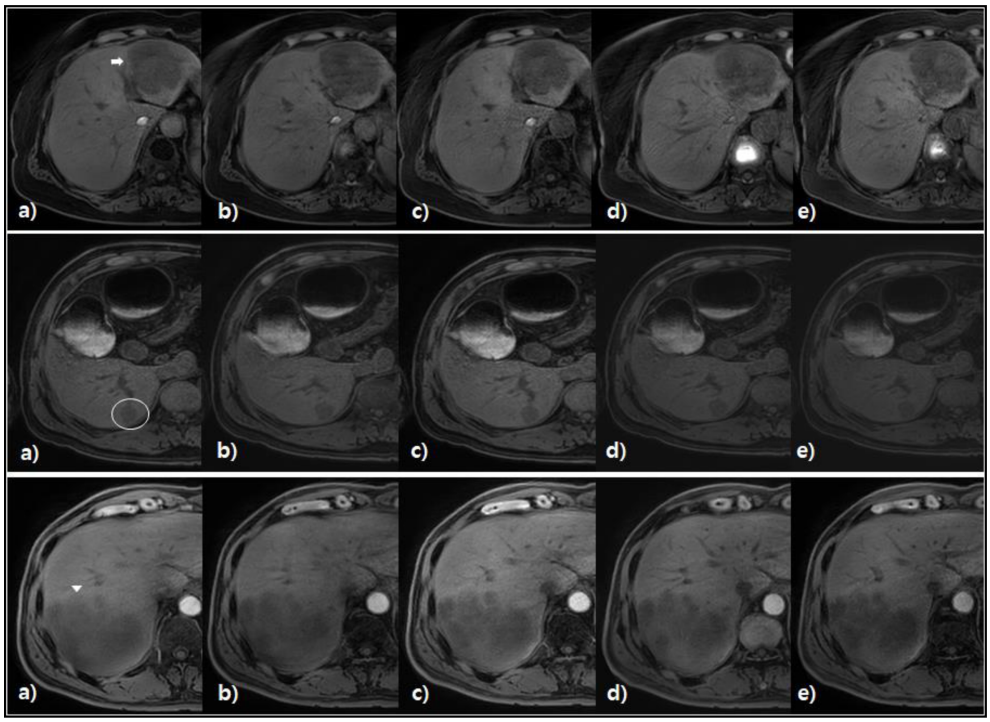

Fig. 6. 3D-mDixon Pre Contrast images with HCC (⇨), Metastasis (○), Abscess (△) according to Five Flip Angle of 11° (a), 14° (b), 17° (c), 20° (d) and 23° (e).

[16]. Also, it has more excellent soft tissue contrast than CT image does and can provide more diagnostic information. And yet, in the existing abdominal MRI scan, image quality may fall by Motion Artifact due to breath. To reduce that, the patient should continuously suppress breath, and it may cause a fatal error in reading due to the artifact [17]. In the preceding studies to find the optimum flip angle with BH technique, it was reported that SNR and CNR were the highest in the image at 10° out of those at 5°, 10°, 15°, 20°, and 25° and decreased after 15° [18]. Since the BH technique has a short test time of about 15-19 seconds, in the equation to calculate the measured value, scan time was not considered while in this study, since it took minutes to test, the equation including scan time was used in calculating SNR and CNR to get the accurate measured value. SNR and CNR values of the liver were: 5°: 55.00 ± 12.61, 30.50 ± 3.84, 10°: 140.08 ± 19.18, 43.00 ± 5.42, 15°: 102.63 ± 14.25, 36.54 ± 4.09, 20°: 86.15 ± 13.91, 32.30 ± 2.79, and 25°: 74.61 ± 13.65, 31.69 ± 3.21, the highest at 10°. 3D VANE XD applied in this study was 143.63 ± 16.16, 92.23 ± 11.34 at 17°, and SNR value was a little higher than the existing technique, while CNR value was about two times higher. Overall, this research technique obtained higher results with HCC diseases, as well, and 3D VANE XD using FA of 17° was more excellent than the result values [19, 20]. especially, in the ranges of 15° and 20°.

In the latest model applied to this study, with the 3D VANE XD technique, the abdominal examination can be conducted while the patient can freely breathe to overcome these disadvantages, which can enhance image quality [21]. There are factors affecting the quality of the MRI image, including SNR, CNR, spatial resolution, and Scan Time, and since they have correlations with each other, it is necessary to control them appropriately.

This correlation and parameter change can make high signal intensity; however, they lead to an increase in Specific Absorption Rate (SAR), as well, which may cause an increase in body temperature. Thus, the optimum flip angle (FA) is required. SAR is affected by the conductivity and tissue density, etc. of the target substance, which can be shown like the following equation (Eq. 8) [22].

$$\mathrm{SAR} = \int \frac{\sigma(|E_x|^2 + |E_y|^2 + |E_z|^2)}{2\rho} dV, \tag{8}$$

σ: Material conductivity,
ρ: Tissue density,
$E_{x,y,z}$: Amplitude of orthogonal component of the electric field.

In the previous research results, in the T1 GRE image, since SAR increases in proportion to flip angle, it is

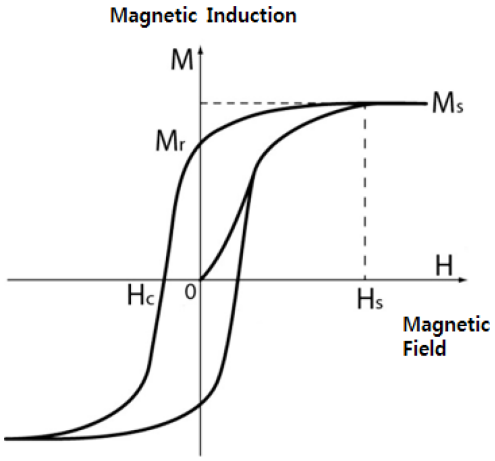

Fig. 7. Schematic Showing magnetic Hysteresis Loop, The area of Hysteresis Loop is rerated to energy dissipation upon reversal of the field.

necessary to select the optimum parameter applicable to the clinic [23]. Primovist® used in Liver MRI is a magnetic substance, which shortens T1 and T2 relaxation time, changing the susceptibility between tissues and shows the tissue with a higher signal intensity than that of other tissues. At this time, in electromagnetics, the relationship between the magnitude of the external magnetic field and the induced susceptibility is defined like the following equation (Eq. 9) [24].

$$B = \mu_0(H + M) = \mu_0(H + xH) = \mu_0(1 + x)H + \mu H, \quad (9)$$

B : External magnet field,
μ : Permeability in vacuum,
μ_0 : Permeability in material,
H : Magnet field strength in material.

Besides, for most magnetic materials, magnetization greatly differs depending on the magnitude and direction of the external magnetic field when the external magnetic field applies, and it has a unique property that follows a hysteresis loop like Fig. 7 [25]. Primovist® is a hepatocyte-specific contrast medium, and the most important factor for the hepatocyte intake mechanism is the Organic Anion Transporting Polypeptide8 (OATP8) translocator [26]. The contrast medium taken in hepatocytes is discharged through the biliary tract by Multidrug Resistance Associated Protein2 (MPR2) translocator, and 50 % of the contrast medium are excreted through the kidney while the other 50 % are taken in hepatocyte and excreted through the bile. Thus, it is possible to get a dynamic contrast-enhanced image and an HBP image together [27]. This study would check the optimum flip angle value through quantitative and qualitative evaluations, applying five flip angles in acquiring an image before the contrast medium injection and HBP image, using 3D VANE XD technique. As a result of a comparison of MRI images at five flip angles before the contrast medium injection, SNR and CNR were the highest in the image at the flip angle of 17° in the quantitative analysis, and the higher flip angle, the more measured value became, and then, it decreased after 17°. In addition, in the qualitative analysis, the image at 17° had more excellent hepatic parenchymal and blood vessel intelligibility than those of other control groups. Likewise, in the HBP imaging evaluation, experiments were conducted, applying five flip angles from 11° at an interval of 3° to HCC, Metastasis, and Liver Abscess disease.

Like the imaging evaluation before the contrast medium injection, in the HBP image, CNR was the highest in the lesion and normal regions in the image at the flip angle of 17°, and in the qualitative evaluation, liver blood vessel intelligibility and localized lesion clarity had excellent results. In the 3D T1 fat-suppressed GRE image, the longitudinal magnetization is imperfectly recovered due to short TR. This effect can increase the contrast between two tissues in the HBP image as it increases the signal intensity of the contrast-enhanced tissue with short T1 relaxation time with the increase of flip angle and decreases that of the lesion with long T1 relaxation time, in which no contrast medium was taken [28]. It was found that at a flip angle higher than 20°, SNR and CNR decreased, and this is because the higher the flip angle, the higher the background noise becomes. As for a limitation of this study, the 3D VANE XD technique had an advantage that it would not be affected by motion artifact since the patient should not suppress breath, while it was hard to analyze the artery phase image since it took minutes more scan time than the existing BH technique. And yet, it is a useful technique for patients who had had difficulty in having liver MRI when a study was conducted with hypovascular diseases and can provide the optimum clinical information for all patients if the BH technique and FBH (3D VANE XD) technique are used selectively for their conditions.

5. Conclusions

In conclusion, free breath-hold images in the hepatobiliary phase applying the 3D VANE XD technique, the image applying the flip angle of 17° could get an image with overall better quality than others applying different flip angles as well as helping understand the characteristics of the lesion. In a liver MRI scan, for the patient who is unconscious or has difficulty in communication due to

disability, it is expected that conducting a test, applying the flip angle of 17° using 3D VANE XD technique, while the patient breathes freely without suppressing breath, would increase the image quality and decrease the artifact due to motion to help understand the characteristics of the lesion.

Conflicts of Interest

No potential conflict of interest relevant to this article was reported.

References

[1] R. L. Siegel, K. D. Miller, and A. Jemal, CA Cancer J. Clin. **70**, 7 (2020).
[2] M. J. Kim, J. Korean Med. Assoc. **56**, 948 (2013).
[3] G. Wang, S. Zhu, and X. Li, Oncol. Lett. **17**, 1184 (2019).
[4] J. A. Luetkens, P. A. kupczyk, J. Doemer, R. Fimmers, W. A. Wilinek, H. H. Schild, and G. M. Kukuk, Eur. Radiol. **25**, 3207 (2015).
[5] J. H. Yoon, J. M. Lee, M. H. Yu, E. J. Kim, J. G. Han, and B. I. Choi, Abdomen Imaging **39**, 711 (2014).
[6] E. H. Goo, J. Korean Soc. Radiol. **13**, 271 (2019).
[7] S. Currie, N. Hoggard, I. J. Craven, M. Hadjivassiliou, and I. D. Wilkinson, Postgrad Med. J. **89**, 209 (2013).
[8] G. Helms, H. Dathe, and P. Dechent, Magn. Reson. Med. **89**, 667 (2008).
[9] H. H. Park, E. H. Goo, I. C. Im, J. S. Lee, M. J. Kim, B. J. Kwak, W. K. Chung, and K. R. Dong, J. Korean Phys. Soc. **61**, 1866 (2012).
[10] R. K. Yang, C. G. Roth, R. J. Ward, J. O. deJesus, and D. G. Mitchell, Radiographics **30**, 185 (2010).
[11] D. M. Hedderich, K. Weiss, J. E. Spori, D. Giese, G. M. Beck, D. Maintz, and T. Perdigehl, Rofo. **190**, 601 (2018).
[12] T. A. Gallagher, A. J. Nemeth, and L. Hacein-Bey, AJR Am J. Roentgenol. **190**, 1396 (2008).
[13] W. K. Jeong, Y. K. Kim, K. D. Song, D. G. Choi, and H. K. Lim, Clin. Mol. Hepato. **19**, 360 (2013).
[14] S. S Kim, J. Y. Choi, and H. J. Rhee, J. Korean Soc. Radiol. **85**, 374 (2019).
[15] U. Motosugi, P. Bannas, C. A. Bookealter, K. Sano, and S. B. Reeder, Radiology **279**, 93 (2015).
[16] J. T Campos, C. B. Sirlin, and J. Y. Choi, Insights Imaging **3**, 451 (2012).
[17] I. Havsteen, A. Ohlhues, K. H. Madsen, J. D. Nybing, H. Christensen, and A. Christensen, Front Neurol. **30**, 232 (2017).
[18] K. R. Dong, E. H. Goo, J. S. Lee, W. K. Chung, and Y. J. Kim, J. Korean Phys. Soc. **64**, 1202 (2014).
[19] E. H. Goo, D. C. Kwon, K. R. Dong, J. S. Lee, W. K. Chung, J. W. Choi, J. W. Lee, and C. H. Choi, Appl. Magn. Reson. **40**, 221 (2011).
[20] B. W. Lee, M. C. Park, J. H. Lee, K. J. Kim, and S. H. Bae, Journal of Digital Convergence, **12**, 385 (2014).
[21] K. A. Jang, Y. K. Kim, E. J. Kim, W. K. Jeong, D. G. Choi, W. J. Lee, S. H. Jung, and S. Y. Baek, Korean J. Radiol. **16**, 1038 (2015).
[22] C. M. Collins and Z. Whang, Magn. Reson. Med. **65**, 1470 (2011).
[23] J. B. Han, S. H. Hong, N. G. Choi, and H. J. Seong, JKCA. **13**, 308 (2013).
[24] G. Parigi, E. Ravera, and C. Luchinat, Prog. Nucl. Magn. Reson. Spectroscopy **114**, 211 (2019).
[25] C. Louizos, J. A. Yanez, M. L. Forrest, and N. M. Davies, J. Pharm. Sci. **17**, 34 (2014).
[26] J. Y. Choi, J. M. Lee, and C. B. Sirlin, Radiology **273**, 30 (2017).
[27] A. Kitao, O. Matsui, N. Yoneda, K. Kozaka, R. Shinmura, W. Koda, S. Kobayashi, T. Gabata, Y. Zen, T. Yamashita, S. Kaneko, and Y. Nakanuma, Eur. Radiol. **21**, 2056 (2011).
[28] H. Haradome, L. Grazioli, K. Almanea, M. Tsunoo, U. Motosugi, T. C. Kwee, and T. Takaraha, J. Magn. Reson. Imaging **35**, 1132 (2012).